A COMPACT ISOLATION FRAME FOR MITIGATING PACKAGING STRESS AND ANCHOR LOSS IN MICROACOUSTIC RESONATORS

Maliha Sultana, Tanvir Hasan, Jennyfer Vivas Gomez, Kevin Chan, Hakhamanesh Mansoorzare, and Reza Abdolvand
University of Central Florida, Orlando, Florida, USA

ABSTRACT

In this work, the effectiveness of compact isolation frames in mitigating the stress-induced frequency shifts and concurrently boosting the quality factor (Q) of piezoelectric MEMS resonators is studied. Piezoelectric MEMS resonators are a promising candidate for replacing Quartz and capacitive resonators for timing applications. However, many classes of such resonators have multiple anchor points which makes them susceptible to failure due to packaging induced stress. In this work, by introducing tailored trenches around said resonators and experimentally comparing their performances with baseline devices, it is shown that the stress-induced frequency shifts could be reduced by up to ~94%. This is further validated by optical profiling that shows reduced device curvature. Moreover, compared to the baseline resonators, the isolation frame boosts the Q of the devices by up to 2.9x while minimally impacting the device footprint. Consequently, the isolation frame could facilitate commercialization of piezoelectric MEMS clocks by addressing packaging stress issues.

KEYWORDS

MEMS resonator, packaging stress, stress isolation frame, thickness-Lamé mode.

INTRODUCTION

MEMS resonators are replacing quartz counterparts for timing applications and capacitive MEMS resonators are currently commercially available [1]. The weak electromechanical coupling in capacitive MEMS resonators, however, results in higher loss and limits their application in low power scenarios. To overcome the weak coupling issue, a viable solution is piezoelectrically exciting/detecting the vibration of a single crystal MEMS resonator, as shown in thin-film piezoelectric-on-silicon (TPoS) platform [2]. A great challenge towards commercializing this platform is the packaging and packaging induced stress in the resonant body that could cause frequency drifts and clock instability. Packaging of MEMS device enables physical interfacing of the device with the environment. Even if the challenges associated with external environment (e.g. moisture, temperature) are ignored, there are inherent obstacles within the MEMS packaging. These includes aspects such as die handling, die attach procedures, interfacial stress management, and outgassing due to poor encapsulation [3]. The die attachment material used in packaging has its own compliance and flexibility to absorb and distribute mechanical stress. When the MEMS resonator is subjected to differential pressure, the die attachment material may compress or deform, leading to uneven distribution of pressure across the resonator. This uneven distribution can induce mechanical stress on the resonator structure and affect its performance, for example, by shifting the resonance frequency [4]. This impact is exacerbated by having two or more anchoring points to the substrate that suspend the resonant body (Figure 1). Therefore, mitigating the stress translation in a compact manner within a simple packaging is critical for building reliable clocks in this platform at commercial scale.

Several studies have been reported previously to reduce packaging stress impact on the resonant body. One aspect of stress-free packaging uses die attaching adhesive with high die shear strength for bonding the MEMS chip securely to the substrate [5]. Using this adhesive with high flexibility and low curing temperature reduces the effect of stress development during temperature changes. In addition, stress isolation structures to suppress the effect of packaging stress in silicon on insulator (SOI) based MEMS devices have shown promising outcomes [6] [7]. The addition of the supporting frame effectively eliminates the uneven distribution of thermal stress and deformation on the device. However, the additional structure may introduce mechanical constraints or interference, and add to the fabrication complexity.

In this work, a new isolation frame is introduced to surround the MEMS resonator for mitigating stress-induced deformation or bending of the resonant body. Diverging from prior research, the proposed method stands out for its compact design and minimal footprint as well as eliminating the necessity for any additional fabrication steps, thus less resource intensive. Moreover, since the regions surrounding the anchors of the resonator impact its anchor loss, the proposed isolation frame could be geometrically optimized to reduce such losses. To replicate packaging stress on the resonator, die attach epoxy is used to mount the resonator die onto a custom PCB bending setup while measuring the frequency response of the device. The asymmetric packaging stress is evaluated by measuring the bended angle of the resonant body using an Optical Profiler. Experimental results validate the stress-suppression effect in the resonators with isolation frame in comparison to the baseline resonators. Notably, the isolation frame not only reduces the stress-induced frequency drifts in the resonator, but it also enhances the resonators quality factor (Q) by reducing losses due to irreversible energy leakage to the substrate through the anchors. In the following sections the design, fabrication, and measurement technique/results are discussed.

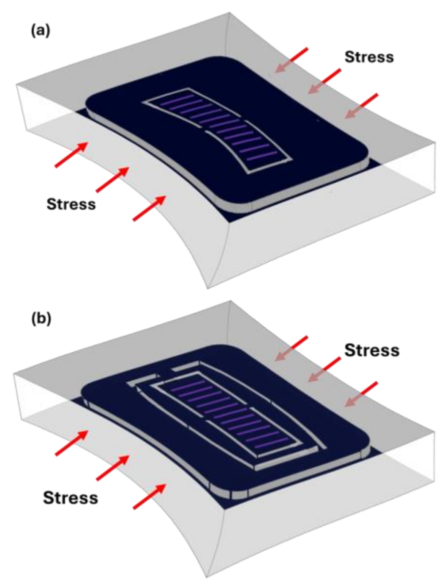

Figure 1: Illustration of packaged MEMS resonator, highlighting the impact of induced stress. (a) Baseline resonator; (b) Resonator with Isolation Frame.

978-1-940470-05-4/HH2024/$25©2024TRF
DOI 10.31438/TRF.HH2024.109

DESIGN & FABRICATION

The resonators used in this study are thickness-Lamé mode (TLM) which is realized once the resonator thickness approaches the half wavelength (Figure 2). Auxiliary trenches are added around the resonator to create a single point of substrate connection for stress relief while the footprint was kept as compact as possible by keeping the trenches adjacent to the resonant body. TLM offers low thermoelastic damping and its dominant source of loss is from the anchors due to absence of cross-sectional nodal points [8], [9]. To reduce the radiation of energy into the substrate through anchors, first the dimension of the resonator is optimized using COMSOL Multiphysics finite element analysis (FEA). Changing the dimensions however has limited impact due to the absence of zero displacement region across the entire thickness where the anchors are located. Therefore, it is critical for the stress isolation frame to also function as an in-plane acoustic reflector. This could reduce the need for large structures such as phononic crystals used for reducing the anchor loss in this platform [10]. Since the size of the resulting acoustic cavity formed by the isolation frame affects the anchor loss [11], its dimension was chosen so that the maximum amount of radiated acoustic energy can be reflected back from the edge of the frame to the resonator. Figure 3 shows the simulation results for the anchor quality factor as a function of the frame edge distance from a point on the anchor. The FEA model includes the stack of piezoelectric material which is aluminum nitride (AlN), and single crystalline silicon (Si) and it integrates two domains, namely structural mechanics and electrical, by coupling them using the piezoelectric layer. Low reflecting boundary condition is applied at the die edges to capture the anchor loss.

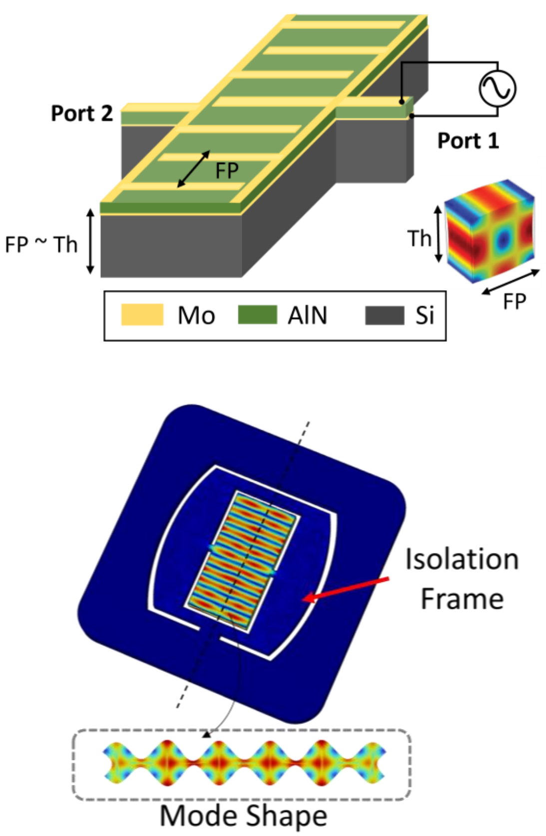

Figure 2: Conceptual schematic of a thickness-Lamé mode resonator (top) and its resonance mode shape (displacement) simulated by COMSOL (bottom).

To empirically analyze the effectiveness of the isolation frames, sets of resonators were designed with multiple configurations of tethers, with and without isolation frame. As expected, in terms of anchor Q, the simulations show the device with a single pair of tethers has higher Q than the devices with multiple tether pairs since the presence of multiple tether pairs introduces additional mechanical coupling points between the resonator and the substrate at displacement nodes. Furthermore, while these tethers are intended to provide structural support and stability, they can inadvertently create regions of stress concentration which is experimentally investigated in this work. This concentration of stress can lead to localized deformation or failure, especially close to the tether regions, under mechanical or thermal loading. Consequently, the resonators with multiple number of tethers are expected to show larger frequency shift than the baseline single tether devices.

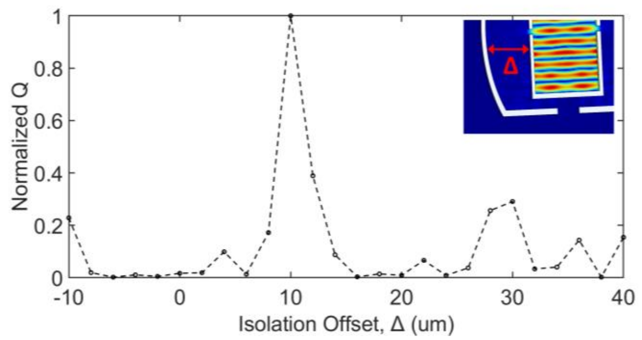

Figure 3: Normalized anchor Q vs isolation frame offset from the anchor (as shown in the schematic) simulated by COMSOL. The data points are marked and the dashed line is for visual aid.

The set of TLM TPoS resonators with different configurations are fabricated on a 21 um SOI wafer with a stack of Molybdenum (Mo)-AlN-Mo thin film. The AlN layer is 1 um thick and sandwiched between 100 nm Mo layers. The process starts with the dry etching of top Mo layer in an SF6/O2 plasma to pattern the top electrodes (Figure 4a). The next step is to the access to the bottom metal through the AlN layer (Figure 4b). AlN is wet etched in a heated TMAH based solution. A thin layer (100 nm) of gold is lifted off on the pad connection to create better ohmic contact (Figure 4c). The resonator body is formed by the full stack etching (AlN-Mo-Si) down to the buried oxide (BOX) layer by two consecutive steps of plasma etching in inductively coupled plasma (ICP) and deep reactive ion etching (DRIE) process (Figure 4d). The Si handle layer at the backside is then etched in DRIE process to reach the etch stop BOX layer. Finally, the resonator is released by wet etching the BOX in buffered oxide etchant (Figure 4e).

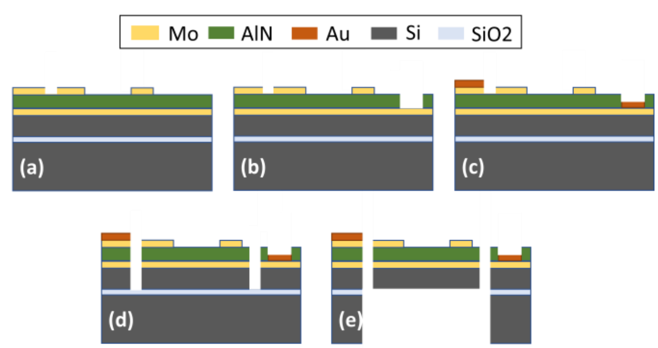

Figure 4: Simplified fabrication process flow of the TLM resonator.

MEASUREMENT

The set of resonators having different configurations are characterized by measuring their 2 port frequency response using a network analyzer (Rhode & Schwarz ZNB 8) and a pair of GSG microprobes. Figure 5 shows the measured frequency response of a typical fabricated resonator with isolation frame showing its SEM in the inset. The device has a loaded *Q* (measured from the 3dB bandwidth of the transmission response) of 20k and an insertion loss (IL) of 18.4 dB. The *f.Q* product of all the devices is summarized in Table 1.

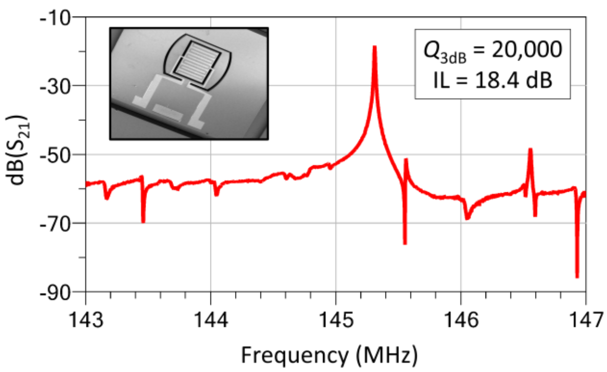

Figure 5: Measured frequency response of a typical thickness-Lamé mode resonator with isolation frame along with its SEM.

Next, the frequency shifts of the resonators under bending test is recorded. The die containing the resonators is affixed to a PCB using an epoxy die attachment, ensuring a secure bond. Said PCB is suspended over another PCB of the same size and supported at four corners with screws. The stress application method involves tightening the screws in a controlled manner so that the upper PCB is bent while the frequency response of the resonator is recorded by microprobes connected to a network analyzer (Figure 6). By comparing the recorded frequency responses with the ones measured before bending the PCB, the frequency shifts due to the bending are obtained.

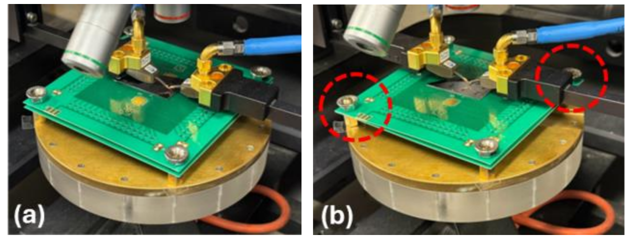

Figure 6: Stress inducing measurement set-up: (a) before bending; (b) after bending (applied stress points are highlighted).

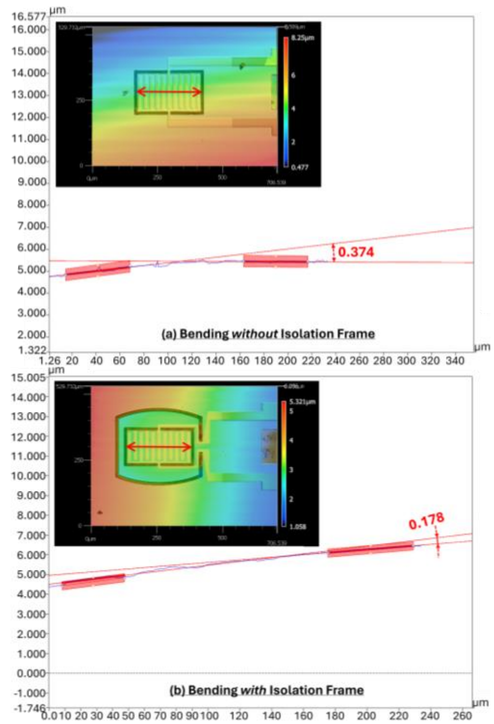

Figure 7: Measured bending angle/curvature of resonator under stress. Inset shows deviation of height from original position across resonators (as measured by optical profiler).

Table 1: Measured f.Q products, frequency shifts (ΔF), and curvatures (K) for different configurations of the devices under study.

Baseline	SEM	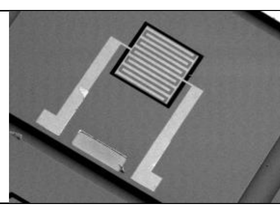	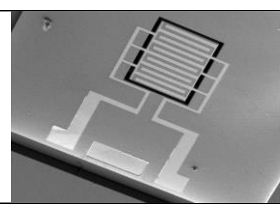	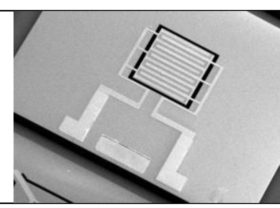
	f.Q (THz)	1.2	0.9	0.8
	ΔF (ppm)	28.23	75.85	125.35
	K (degree)	0.374	0.395	0.249
Isolation Frame	SEM	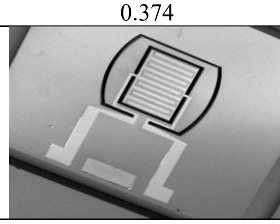	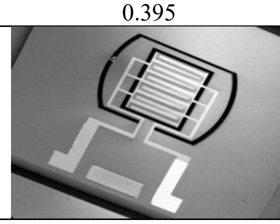	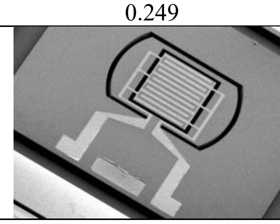
	f.Q (THz)	3.1	2.6	2.5
	ΔF (ppm)	4.58	10.97	7.79
	K (degree)	0.178	0.035	0.132

As summarized in Table I, the bending can cause a maximum frequency shift of 18 KHz (125.35 ppm) in a baseline device while this large frequency shift is reduced to around 1 KHz (7.8 ppm) in a device with the isolation frame (18x reduction). The curvature of the devices (shown for 2 cases in Figure 7) measured using Keyence 3-D Optical Profiler is also summarized in Table I. Similar trend is observed; devices with isolation frame show less bending which implies less impact from stress and deformation. Finally, the effectiveness of the isolation frame in reducing the anchor loss is evident by the higher measured *Q*s compared to baseline devices in all cases. This is while the whole device occupies a footprint of only ~260x320 um^2 which is well within the range of conventional and cost-efficient packaging solutions.

CONCLUSION

In conclusion, this study has demonstrated the significance of compact isolation frames in alleviating potential packaging stress in piezoelectric MEMS resonators. The vulnerability of MEMS resonators, especially the ones with multiple anchor points to the substrate, to packaging-induced stress underscores the necessity for effective mitigation strategies. This stress-induced frequency shifts can be minimized significantly with the addition of tailored trenches around the resonators, as observed in experimental analysis and validated by optical profiling. Moreover, the isolation frames have exhibited the potential to significantly enhance the quality factor of the resonator, with improvements of up to 2.9 times compared to the baseline resonators. This work investigates the impact of these isolation frames on stress-induced frequency drifts, and highlights crucial insights to improve performance towards commercial piezoelectric MEMS resonators for timing applications.

ACKNOWLEDGEMENTS

The authors would like to thank Advanced Modular Systems Inc. for their help with the deposition of AlN films.

REFERENCES

[1] SiTime Corporation, "MEMS Clock Generators," SiTime, [Online]. Available: https://www.sitime.com/products/clock-generators. [Accessed 18 01 2024].

[2] R. Abdolvand, H. M. Lavasani, G. K. Ho and F. Ayazi, "Thin-film piezoelectric-on-silicon resonators for high-frequency reference oscillator applications," *IEEE Transactions on Ultrasonics, Ferroelectrics, and Frequency Control,* vol. 55, pp. 2596-2606, 2008.

[3] C. O'Neal, A. Malshe, S. Singh, W. Brown and W. Eaton, "Challenges in the Packaging of MEMS," in *Proceedings International Symposium on Advanced Packaging Materials. Processes, Properties and Interfaces*, 1999.

[4] H. A. Tilmans, M. Elwenspoek and J. H. Fluitman, "Micro resonant force gauges," in *Sensors and Actuators A: Physical*, 1992.

[5] T. Königer, "New die attach adhesives enable low-stress MEMS packaging," in *36th International Electronics Manufacturing Technology Conference*, 2014.

[6] Y. Hao, W. Yuan, J. Xie, Q. Shen and H. Chang, "Design and Verification of a Structure for Isolating Packaging Stress in SOI MEMS Devices," *IEEE Sensors Journal,* vol. 17, no. 5, pp. 1246-1254, 2017.

[7] X. Wang, D. Xiao, Z. Hou, Q. Li, Z. Chen and X. Wu, "Temperature robustness design for double-clamped MEMS sensors based on two orthogonal stress-immunity structure," in *Proc. IEEE SENSORS*, 2015.

[8] R. Tabrizian, A. Daruwalla and F. Ayazi, "High-Q energy trapping of temperature-stable shear waves with Lamé cross-sectional polarization in a single crystal silicon waveguide.," in *Applied Physics Letters 108.11*, 2016.

[9] S. Sarah, H. Mansoorzare, A. Mahigir and R. Abdolvand, "Thickness-Lamé thin-film piezoelectric-on-silicon resonators," *Journal of Microelectromechanical Systems,* vol. 29, no. 3, pp. 296--305, 2020.

[10] S. Dabas, D. Mo, B. Chatterjee and R. Tabrizian, "Ultra-High Q Self-Ovenized AlScN-On-Si X-Lamé Resonator For Stable Clock Generation," in *IEEE International Conference on Micro Electro Mechanical Systems*, Texas, 2024.

[11] H. Mansoorzare, S. Moradian, S. Shahraini, R. Abdolvand and J. Gonzales, "Achieving the Intrinsic Limit of Quality Factor in VHF Extensional-Mode Block Resonators," in *2018 IEEE International Frequency Control Symposium (IFCS)*, 2018.

CONTACT

M. Sultana, tel: +1-407-534-0144; Maliha.sultana@ucf.edu